Macromolecules

Article

pubs.acs.org/Macromolecules

Cross-Linked Block Copolymer/Ionic Liquid Self-Assembled Blends for Polymer Gel Electrolytes with High Ionic Conductivity and Mechanical Strength

Daniel F. Miranda, Craig Versek, Mark T. Tuominen, Thomas P. Russell,* and James J. Watkins*

Department of Polymer Science and Engineering Department of Physics, University of Massachusetts Amherst, Massachusetts 01003, United States

Supporting Information

ABSTRACT: Poly(propylene oxide)−poly(ethylene oxide)−poly(propylene oxide) (PPO−PEO−PPO) block copolymers (BCPs) with cross-linkable end groups were synthesized, blended with an ionic liquid (IL) diluent, and cross-linked to form polymer gel electrolytes. The IL prevented crystallization of PEO at high concentrations, enabling fast ion transport. In addition, the IL was selective for the PEO block, inducing strong microphase separation in what are otherwise disordered or weakly ordered BCP melts. Cross-linking the BCPs in the presence of the IL resulted in the formation of solid, elastic gels with high ionic conductivities—greater than 1.0 mS/cm at 25 °C for some compositions. However, it was found that neither the presence or absence of microphase separation nor the BCP composition of the microphase separated gels substantially influenced ionic conductivity. Increasing the cross-link density through the use of phase-selective PEO- and PPO-based cross-linking reagents was also evaluated. It was revealed that confinement of cross-links to the PPO rich domains through the use of PPO-based diacrylates enhanced the mechanical strength of the gels without detriment to the ionic conductivity. Conversely, cross-linking in the PEO-rich domains through the use of PEO-based acrylates significantly reduced conductivity. Isolation of cross-links within a minor nonconducting domain in a microphase separated gel is a viable strategy for mechanical property enhancement without a large sacrifice in conductivity, effectively decoupling ionic conductivity and mechanical strength. This approach yielded solid-like gel electrolytes fabricated from BCPs that can be produced inexpensively, with ionic conductivities of 0.64 mS/cm at 25 °C and a frequency independent storage modulus of approximately 400 kPa.

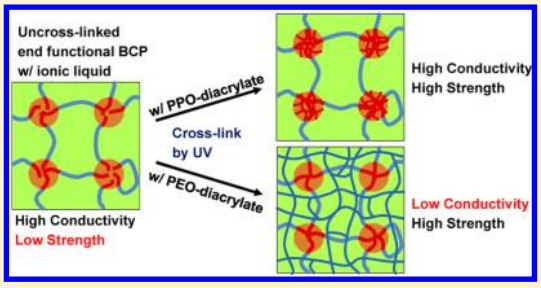

INTRODUCTION

Solid polymer electrolytes are ion-conducting media composed of polymers that are capable of coordinating with and transporting charged molecules. These materials have many desirable characteristics for applications such as anion and proton exchange membranes in fuel cells,[1] electrolyte layers in dye-sensitized solar cells,[2] as separators in capacitors,[3] and electrolyte layers in lithium batteries.[4,5] In particular, there are many benefits to using solid polymer electrolytes in place of the conventional liquid electrolytes in lithium ion batteries. These advantages include reduced flammability by the elimination of flammable organic solvents used in liquid electrolytes and also the capacity to construct electrolytes as thin films, leading to greater energy density in batteries.[4]

Unfortunately, the ionic conductivity of solid polymer electrolytes is generally quite poor, well below the 1.0 mS/cm (at 25 °C) minimum required for a practical battery electrolyte.[6,7] One reason is the high crystallinity of most ion-coordinating polymers. It was established very early in the development of polymer electrolytes that polymer crystallization suppresses ionic conductivity.[8,9] More recent work has established a clear correlation between polymer segmental dynamics and ion transport.[10] In addition, stoichiometric polymer/salt complexes can form in mixtures of lithium salts and ion-coordinating polymers, decreasing ionic conductivity due to the increased physical restraints imparted by these complexes.[9,11] Therefore, to achieve fast ion transport, a diluent is required to plasticize the polymer and ensure complete lithium salt disassociation. Such polymer gel electrolytes should have superior performance to all-solid polymer electrolytes.

Room temperature ionic liquids (ILs) are a very promising class of diluents for the fabrication of polymer gel electrolytes. Room temperature ILs are salts of organic cations and anions with low melting temperatures (<25 °C), negligible vapor pressure, and have thermal and electrochemical stability superior to most organic solvents.[12] As such, replacing flammable organic solvents used in liquid electrolytes or polymer gel electrolytes[13−15] with low-flammability ILs would allow for the construction of batteries with reduced fire hazards. ILs also have the capacity to plasticize ion-coordinating polymers[16,17] and to dissolve lithium salts,[18] promoting fast

Received: June 29, 2013
Revised: October 6, 2013
Published: November 26, 2013

ion transport. ILs have been used on many occasions as diluents for polymer gel electrolytes.[16,17,19−21]

However, if the polymer is fully plasticized by an IL diluent, it will behave as a polymer solution or melt and cannot form a mechanically stable film as required for a thin film electrochemical cell. To counter this, several methods have been explored to provide mechanical support to IL/polymer gel electrolytes. These methods include polymerizing a polymer in an IL solution along with a cross-linking comonomer,[22,23] swelling poly(vinylidenefluoride-*co*-hexafluoropropylene) random copolymers in an IL to make a physical gel,[24−26] and chemical cross-linking of poly(ethylene oxide) (PEO) blended with an IL.[27−31]

Many studies have also investigated the use of block copolymers (BCPs) for polymer electrolytes,[32−49] as well as mixtures of BCPs with IL diluents or BCPs incorporating polymerized ionic liquids.[50−62] BCPs consist of two dissimilar polymer chains (blocks) linked together by a covalent bond. When the repulsive interactions between the component blocks are sufficiently large, the blocks phase separate on a nanometer scale (historically termed microphase separation) into well-defined, periodic nanostructures.[63,64] It has been suggested that BCP microphase separation creates well-defined ion conducting channels, and indeed several reports have shown that control over BCP morphology and microdomain orientation can be used to enhance ionic conductivity.[38,54,55,60,61] Strong microphase separation[35,36,47,57,58] and large microdomain width[35,39] also favor high conductivity. In addition, by using a BCP consisting of both an ion-conducting block and a rigid block, it may be possible to obtain both high conductivity and high mechanical strength.[35,43,49,52] This would be a significant development, as there is typically a trade-off in polymer electrolytes between ionic conductivity and mechanical strength due to the correlation between slow polymer dynamics and reduced ionic conductivity.[10] Microphase separation of an ion-conducting block and a reinforcing block reportedly allows ionic conductivity and mechanical strength to be decoupled, allowing this trade-off to be avoided.[39,52]

However, it is not universally reported that BCP microphase separation is beneficial for ion transport and polymer electrolyte applications in general. A few reports have concluded that controlling the BCP morphology has no effect on ionic conductivity.[40,53,62] In addition, transitioning from an ordered BCP morphology to a disordered system was also found to have little measurable effect on conductivity.[40] Further work is therefore required to determine the optimal function of BCPs in electrolyte applications.

In this work, the potential benefits of using BCPs for IL containing polymer gel electrolytes were assessed by evaluating the performance of cross-linked IL/polymer gels with varying phase behavior. Gels fabricated from homopolymers with only a single phase, from low molecular weight BCPs having weak microphase separation, and from higher molecular weight BCPs with strong microphase separation were investigated. The effects of BCP phase behavior on the mechanical properties and ionic conductivity were studied to contribute to the understanding of the role of BCP microphase separation in polymer electrolytes.

In addition, the feasibility of using PPO−PEO−PPO BCPs as polymer electrolytes has been investigated. These polymers can be produced inexpensively on an industrial scale, as demonstrated by BASF's catalog of reverse Pluronic surfactants. We used a sample of a reverse Pluronic (25R4), as well as lab-made analogues that can be made by the same chemistry. The low cost of producing these polymers may prove beneficial for practical implementation as battery electrolytes. The cross-linking strategy used may prove beneficial as well, as covalent cross-links persist up to thermal decomposition, whereas physical cross-links such as those from glassy polymers relax out when the glass transition temperature (T_g) is exceeded.[56]

EXPERIMENTAL SECTION

Materials. The IL used in this work is 1-butyl-3-methylimidazolium hexafluorophosphate ([BMI][PF_6]), obtained from Sigma-Aldrich. PEO having M_n equal to 4600 g/mol (PEG 4600) and 8000 g/mol (PEG 8000) were also purchased from Sigma-Aldrich. Pluronic 25R4 was donated from BASF. Synthesis and distillation reagents were all obtained from Sigma-Aldrich: propylene oxide, calcium hydride (CaH_2), potassium hydride (KH, in mineral oil), 12.0 M hydrochloric acid (HCl) 18-crown-6, methacryloyl chloride, triethylamine (TEA), sodium metal (in mineral oil), and benzophenone. All solvents were purchased from Fisher Scientific. A radical inhibitor 4-hydroxy-2,2,6,6-tetramethyl-1-piperidine-1-oxyl (4-OH−TEMPO) was also purchased from Fisher. Cross-linking oligomers, poly(propylene glycol) diacrylate (M_n = 800 g/mol) and poly(ethylene glycol) diacrylate (M_n = 700 g/mol) were purchased from Sigma-Aldrich. A free-radical generating photoinitiator, 2,2-dimethoxy-2-phenylacetophenone was also purchased from Sigma-Aldrich.

Tetrahydrofuran (THF) was distilled over a sodium/benzophenone ketyl still prior to use. Propylene oxide was vacuum distilled over calcium hydride. Prior to use, the mineral oil was removed from KH by mixing the slurry with distilled THF, followed by gravity filtration. 18-crown-6 was dried under vacuum at 70 °C for 20 h. TEA was distilled over CaH_2. The cross-linkable poly(ethylene oxide) and poly(propylene oxide) oligomers were stripped of inhibitor by passage through a plug of activated basic alumina. The purified oligomers were stored in a 4 °C refrigerator until required. All other reagents were used as received. Caution must be used when handling sodium metal, CaH_2, and KH as these reagents are all highly reactive with water.

BCP Synthesis. In this work, IL/polymer blends were made from three different PPO-*b*-PEO-*b*-PPO triblock copolymers and from the PEG 8000 homopolymer. Low molecular weight BCPs are commercially available, in the form of Pluronic 25R4 (M_n = 3600 g/mol, 0.40 PEO). Higher molecular weight PPO-*b*-PEO-*b*-PPO copolymers are not commercially available, and had to be synthesized. These BCPs were prepared from PEO macroinitiators with terminal hydroxyl end groups, using KH to activate the end groups and 18-crown-6 as a phase transfer catalyst. Polymerization of propylene oxide was then carried out by anionic ring-opening polymerization from these end groups. Detailed procedures are contained in the Supporting Information section.

The characteristics of the synthesized and the purchased polymers are summarized in Table 1. For the BCPs, BASF's naming convention for Pluronic was employed: the first two digits multiplied by 100 is the combined M_n of the PPO blocks, "R" indicates "reverse" as PPO comprises the end blocks, and the last digit multiplied by 10 is the weight fraction of PEO. The molecular weight and composition of the BCPs was determined by ^{1}H NMR. The dispersity of all the polymers was measured by GPC (THF, polystyrene standard).

Table 1. Characteristics of the Polymers Used in This Work[a]

polymer	total M_n (g/mol)	weight fraction PEO	dispersity
25R4	3600	0.40	1.02
64R4 (lab-made)	11000	0.42	1.02
45R6 (lab-made)	12500	0.64	1.03
PEG 8000	8000	1.00	1.02

[a]"Lab-made" indicates the polymer was synthesized on the laboratory scale. The others were obtained from chemical suppliers.

dx.doi.org/10.1021/ma401302r | *Macromolecules* 2013, 46, 9313−9323

Polymer End-Group Modification. The polymers used in this work were made cross-linkable by replacing the terminal hydroxyl end groups with methacrylates. This was achieved by esterification with methacryloyl chloride (Supporting Information for details). A similar strategy has been used to form hydrogels[65−67] and shape-persistent vesicles[68] from Pluronic surfactants[66,67] and other amphiphiles.[65,68] The end-modified polymers were susceptible to autocross-linking, and were thus stabilized with 300−400 ppm of 4-OH−TEMPO. The end-group conversions of the modified polymers were estimated by ^{1}H NMR. PEG 8000 achieved approximately 100% conversion, 93% for 45R6, 87% for 64R4, and 84% for 25R4.

Blend Preparation. IL/polymer and IL/polymer/cross-linker blends were prepared by mixing the components in methanol, a common solvent for all. Each IL/polymer blend was dissolved in 5 mL of methanol, or 10 mL of methanol for the IL/polymer/cross-linker blends, and stirred for 2 h. For each blend, the concentration of photoinitiator was 0.5 wt % with respect to the polymer. The majority of the methanol was removed under airflow for 2 h, then the blends were dried under vacuum at room temperature for 20 h. The dried blends were stored in a freezer. The vials were wrapped in foil to minimize light exposure during blending and storage. The blends are referred to by the parts by weight of the components present, the polymer used, and the type of cross-linker included (if any). For example, "80/20/10 with 45R6/PEO−acrylate" refers to the blends having 80 parts IL, 20 parts 45R6, and 10 parts PEO−diacrylate cross-linker.

Differential Scanning Calorimetry. Differential scanning calorimetry (DSC) measurements were carried out on a Q200 and also a Q2000 DSC from Thermal Analysis, both equipped with a refrigerated cooling system. During an experiment, the samples were first ramped from 40 to 80 °C at a rate of 25 °C/min. They were held there isothermally for 5 min to ensure complete melting of PEO, then cooled at a rate of 5 °C/min to 0 °C. The samples were held isothermally for 60 min to ensure sufficient time for any PEO crystallization to occur. The temperature was lowered to −20 °C, then ramped to 80 °C at 5 °C/minute. All the reported thermograms are from this second heating run. To determine the crystalline fraction, the heat flow output from the calorimeter was normalized by the mass of PEO present in the blend, and then normalized by the melting enthalpy for a particular blend to the heat of fusion for an infinite, perfect PEO crystal (188.9 J/g).[69]

Cross-Linking. The cross-linking reactions were carried out using a Thermal Analysis brand PCA photocalorimetry accessory, operating at a UV wavelength of 365 nm. The UV intensity for each cross-linked reaction was confirmed with a radiometer. For all samples a UV intensity of approximately 120 mW/cm^2 was used, with an exposure time of 6 min. This exposure time was determined based on photocalorimetry experiments, using the same PCA Photocalorimetry Accessory in a modified TA Instruments calorimeter, model Q2000. Using this instrumentation, the heat flow of the cross-linking reaction could be monitored, allowing the required exposure time for complete cross-linking to be determined. Representative plots are shown in the Supporting Information section. The geometry the samples were cross-linked in depended upon the experiment a particular sample was intended for, and will be detailed in the relevant sections.

Small Angle X-ray Scattering. The SAXS experiments were performed at UMass using a Molecular Metrology (Northampton, MA) instrument. A heating stage (Linkam) was used to run the scattering experiments at 80 °C. Sample holders for small-angle X-ray scattering (SAXS) were made from 1.0 mm thick, 5 mm inner diameter steel washers with Kapton film windows, with the IL/polymer blends sandwiched between. For cross-linked blends, a glass slide having a fluorinated release layer was first used in place of one of the Kapton windows, and the sample was then cross-linked by the described exposure procedure. After cross-linking, the glass slide was removed and replaced with a second Kapton window.

Dynamic Mechanical Analysis. Dynamic mechanical analysis (DMA) was used to evaluate the mechanical properties of the cross-linked blends. Samples for DMA were similarly cross-linked in 5 mm diameter washers, having glass slides with fluorinated release layers as the windows and the blend sandwiched in between. The samples were then cross-linked by UV exposure. After cross-linking, the glass slides were removed, and the cross-linked sample freed from the washer cavity. The diameter was reduced to 3 mm by use of a 3 mm hole punch.

The DMA experiments were run on a Thermal Analysis DMA Q800 in a compression geometry, using 15 mm stainless steel top and bottom plates. The DMA was run in a frequency sweep from 0.02 to 10 Hz. For a few samples, 0.03 Hz was the lower limit or 7.9 Hz the upper limit. These sweeps were at a constant strain of 0.1% and a preload force of 0.5 N. The reported dynamic moduli are the average of separate experiments of three samples created at each IL/polymer or IL/polymer/cross-linker composition.

Electrochemical Impedance Spectroscopy. The electrochemical impedance spectroscopy (EIS) technique was used to determine the ionic conductivity of the blends, un-cross-linked and cross-linked. Samples for EIS were prepared by adding the un-cross-linked blends to glass capillary tubes and inserting gold-plated copper electrodes into either end. The geometry of each tube was carefully measured—the area of the tubes was between 1.2 and 1.4 mm^2, and the distance between electrodes was between 7.0 and 11 mm. The conductivity was then measured by EIS. Afterward, these same samples were cross-linked by UV exposure, still in their original capillary tubes. The conductivity was measured again to compare cross-linked and un-cross-linked blends.

The EIS experiments were carried out using a Solartron SI 1260 impedance analyzer, combined with an 18-channel custom multiplexer constructed by Pickering Interfaces, allowing measurements on 8 samples to be run serially, at each frequency. The measurements were carried out in either an ESPEC model BTU-133 or ESPEC model SH-241 environmental chamber. The experiments were run using a 100 mV amplitude over a frequency range of 10^{-1} to 10^7 Hz. Using the environmental chambers, the temperature during an experiment was ramped from 20 to 80 °C at a rate of 0.25 °C/min, then held at 80 °C for 5 h. The temperature was then cooled from +80 °C to −20 °C at a 0.25 °C/min ramp rate. Besides temperature variation, the measurements were carried out under ambient conditions. The reported conductivities are all from the cooling run, and are the average of separate experiments of three to four samples created at each IL/polymer or IL/polymer/cross-linker composition. Cubic interpolation using the Origin 8.0 software was used to estimate the conductivities at 25 °C.

RESULTS AND DISCUSSION

Suppression of Polymer Crystallization. Polymer crystallization must be prevented to achieve high ionic conductivity in polymer electrolytes. Prior work has shown that [BMI][PF_6] forms a strong interaction with the PEO block of PEO−PPO−PEO triblock copolymers, possibly through hydrogen bonding.[70] This and other works have shown that ILs can suppress polymer crystallization of hydrophilic or ionophilic polymers.[16,19,20,70−72]

Figure 1 summarizes the DSC results for the IL/polymer blends. The neat polymers were all crystalline and, except for 64R4, all show a double melting peak which most likely arises from PEO crystallization with varying numbers of integral folds.[73−75] Crystallinity was greater for polymers with higher molecular weight and/or having a greater PEO fraction, and crystallization in those systems was therefore more difficult to suppress. Crystallization was suppressed entirely for the 25R4 and 64R4 at a 50/50 (IL/polymer by weight) blend composition, whereas an 80/20 composition was required to completely suppress crystallization in 45R6 and PEG 8000.

Phase Behavior. The phase behavior of the IL/polymer blends was investigated in order to correlate the BCP microphase separation strength and morphology of the blends with their ionic conductivity and mechanical properties. Low

dx.doi.org/10.1021/ma401302r | Macromolecules 2013, 46, 9313−9323

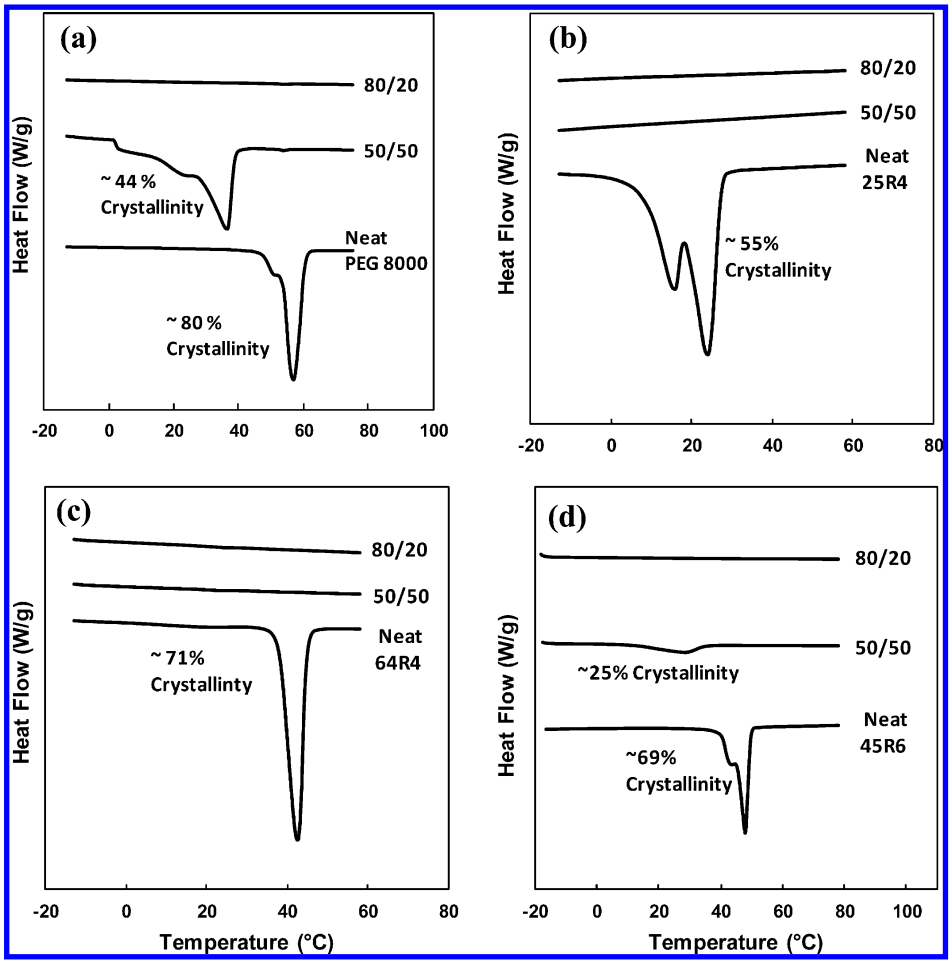

Figure 1. Thermograms of [BMI][PF_6] blends with (a) PEG 8000, (b) 25R4, (c) 64R4, and (d) 45R6.

molecular weight PEO−PPO−PEO and PPO−PEO−PPO triblock copolymers are generally phase mixed above their melting point[70,76] due to the only weakly unfavorable interactions between PEO and PPO.[77] However, prior work has demonstrated that [BMI][PF_6] is strongly selective for the PEO block. This increases the repulsion between PEO and PPO, inducing microphase separation.[70] ILs have been shown to be phase selective for a particular block in amphiphilic BCPs in several other instances.[56,78,79]

This strong phase selectivity was also observed in the present work. Figure 2 shows the SAXS profiles for the neat, un-cross-linked BCPs as well as for the BCP/IL blends, both before and after cross-linking. All SAXS profiles were obtained at 80 °C to prevent PEO crystallization from interfering with the scattering profiles. Neat 25R4 and 64R4 were phase mixed in the melt, but showed clear microphase separation upon addition of the IL due to the selective interaction of the IL with the PEO block. Neat 45R6 appeared to be weakly phase separated, and the separation was dramatically strengthened by addition of the IL.

The SAXS profile for the un-cross-linked 50/50 with 25R4 blend showed a single, very broad peak. Considering that neat 25R4 had no scattering peak, the appearance of a broad peak here indicated that weak microphase separation was induced by blending with the IL. Increasing the IL concentration to an 80/20 composition caused this peak to broaden further, indicating that microphase separation was weakened with further addition of IL.

Narrow primary scattering peaks and several higher order peaks were observed for the un-cross-linked blends with 45R6 and 64R4, indicating strong microphase separation. The 50/50 with 45R6 un-cross-linked blend had a q_1: $3^{1/2}q_1$: $4^{1/2}q_1$: $7^{1/2}q_1$: $9^{1/2}q_1$ ratio of scattering peaks for the first through fifth order peaks, where q_1 is the scattering vector of the primary peak. This is characteristic of a cylindrical morphology, in which the minority domain (PPO) forms cylindrical structures arrayed in a hexagonal pattern in the matrix phase (PEO/IL). The $4^{1/2}$ peak was subdued, likely due to a minimum in the structure factor. The 50/50 with 64R4 un-cross-linked blend had a q_1: $4^{1/2}q_1$: $2.40q_1$ ratio of the first to third order peaks. The third order peak appeared to be distorted; a cylindrical morphology was expected for this composition (approximately 65 vol % assuming complete partitioning of the IL to the PEO microphase), in which case $2.73q_1$ should have been observed. Most likely, this error arose from the weak intensity of the third order peak, making it difficult to accurately locate the peak maximum.

At higher IL concentration, for the 80/20 with 45R6 un-cross-linked blends, there was a q_1: $2^{1/2}q_1$: $3^{1/2}q_1$: $4^{1/2}q_1$ ratio of scattering peaks, indicating a body-centered cubic (BCC) morphology of PPO spheres in a PEO/IL matrix. Peaks for the 80/20 with 64R4 blend had a q_1: $1.6q_1$: $1.9q_1$: $2.5q_1$ ratio of peaks. This ratio does not match any pattern for the established BCP morphologies, although they are close to the pattern expected for a cylindrical morphology (1:1.73:2.0:2.65). It is

dx.doi.org/10.1021/ma401302r | Macromolecules 2013, 46, 9313−9323

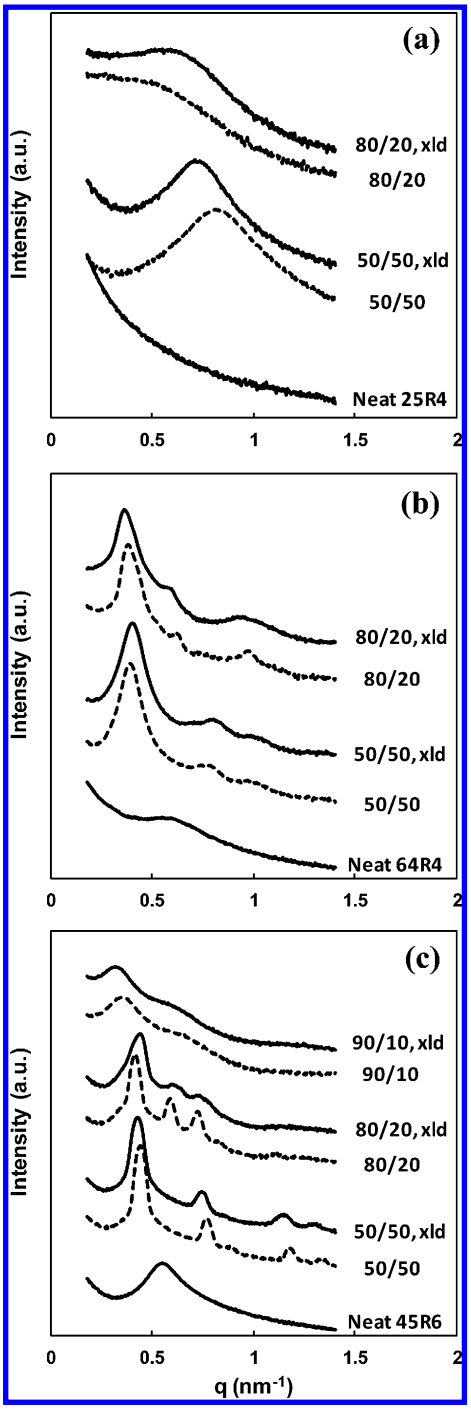

Figure 2. SAXS profiles of the neat BCPs and the BCP/IL blends, both before and after cross-linking (xld), for (a) 25R4, (b) 64R4, and (c) 45R6. All the SAXS profiles were obtained at 80 °C.

possible these peaks represent a distorted hexagonal arrangement of PPO cylinders (discussed below).

For 90/10 with 45R6 blends, there was still a substantial primary scattering peak and a broad second peak, despite the very high IL loading. Therefore, even with 90 parts IL and only 10 parts 45R6, there was still clear microphase separation. When the IL was blended with 25R4 and 64R4 at this concentration, the IL phase separated on a macroscopic scale, most likely due to the smaller fraction of PEO in these BCPs with which to accommodate the IL. For this reason, these blends were not investigated further.

Cross-linking these blends appeared to have a substantial effect on their morphology. For both the 50/50 with 25R4 and 80/20 with 25R4 blends, the scattering peaks sharpened noticeably after cross-linking, indicating that microphase separation was strengthened. It is possible that cross-linking made it more difficult for the PPO and PEO blocks to mix, favoring greater separation. It has also been observed in the literature that cross-linking a BCP in the disordered state can stabilize the ordered state.[80] However, an increase in microphase separation strength was not observed for the higher molecular weight polymers at the 50/50 blend compositions, perhaps because the effect is too weak to be noticed for BCP blends which are already strongly microphase separated. However, for the higher IL concentration 80/20 blends with these polymers, cross-linking caused the primary scattering peaks to broaden and the higher order peaks to combine. It appears that the cross-linking reaction distorted the morphology at higher IL loadings in these polymers.

The possibility of polymer degradation by the UV exposure during cross-linking was eliminated by GPC experiments on BCPs without cross-linking end-groups—there was no change in dispersity or decrease in M_n after UV exposure. The possibility of IL degradation has similarly been examined by NMR before and after UV exposure—the spectra showed no change in the intensity or locations of the IL peaks, indicating that no degradation took place.

It is possible that cross-linking caused a small increase in density for the PPO microdomains, resulting in a volume contraction. At lower IL concentrations (50/50 blends), the relative volume fraction of PPO was larger and thus the PPO blocks were less confined and more able to accommodate this volume change. At higher IL concentrations (80/20), the PPO microdomains occupied a far smaller proportion of the total volume, were more confined, and therefore unable to easily accommodate the volume change. Thus, the shape of the PPO microdomain became distorted, in turn distorting the scattering profile.

Regardless, the primary scattering peak remained fairly sharp and higher order peaks were still observed. Therefore, this broadening does not indicate a weakening of the microphase separation strength upon cross-linking.

Mechanical Properties. Dynamic mechanical analysis (DMA) was used to measure the dynamic storage modulus of the cross-linked blends, the results of which demonstrated that cross-linking the polymers through their end-groups is sufficient to impart mechanical stability to these gels. Only the gels with 80/20 compositions and higher were investigated due to residual crystallinity for some of the 50/50 blends.

Prior to cross-linking, the weakly microphase separated 25R4 blends and the single phase PEO−methacrylate blends were viscous liquids that flow slowly under gravity. The strongly microphase separated blends were quiescent gels that did not flow due to gravity but deformed irreversibly under slight pressures (strongly microphase separated molten BCPs are near a gel point, imparting some solid-like properties[81]). Upon cross-linking, the blends formed solid gels as demonstrated by the DMA experiments shown in Figure 3. Here the compressive storage modulus (G') for each blend was plotted as a function of frequency. Frequency independence has been well established as the primary characteristic of solid-like behavior in polymer gels.[82] The moduli were all largely independent of frequency; the 90/10 with 45R6 blend has the largest dependence of $G' \sim \omega^{0.05}$, which is still essentially

dx.doi.org/10.1021/ma401302r | Macromolecules 2013, 46, 9313−9323

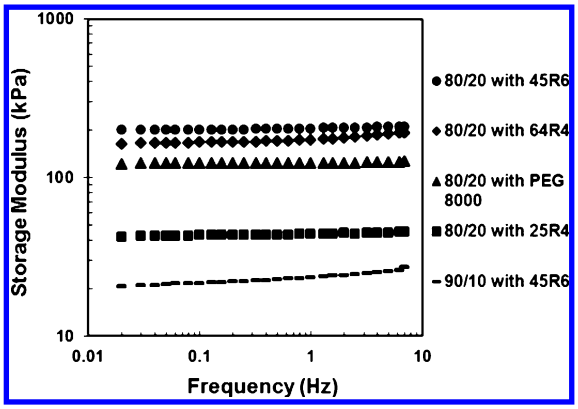

Figure 3. Compressive storage moduli of the cross-linked IL/polymer gels as a function of frequency.

frequency independent. This clearly indicated that cross-linking these blends through the polymer end groups formed solid, elastic gels even at very high IL concentrations, and these gels should be capable of forming mechanically stable electrolyte films.

There were clear differences in the modulus for each composition. The modulus of the 90/10 with 45R6 blend was the lowest (approximately 20 kPa at 0.02 Hz), which was expected as it had the smallest amount of polymer. The differences in moduli between the remaining samples are more difficult to explain. Intuitively, it would be expected that gels with higher cross-link density would have the largest moduli. Therefore, having the lowest M_n and hence greatest cross-link density, the 80/20 with 25R4 gel would be expected to have the highest modulus, followed by 80/20 with PEG 8000, 80/20 with 64R4, and 80/20 with 45R6. However, the opposite trend was observed. The 80/20 with 25R4 blends had the lowest moduli (approximately 40 kPa at 0.02 Hz), followed by the PEG 8000 blends (120 kPa at 0.02 Hz), the 64R4 blends (160 kPa), and 45R6 blends having the highest moduli (200 kPa). One factor may be the difference in phase behavior among 25R4, 64R4, and 45R6. Blends with the higher molecular weight 64R4 and 45R6 BCPs were strongly microphase separated whereas blends with the 25R4 copolymer had very weak microphase separation. The cross-linking end-groups should be in a more concentrated area for a well-defined microdomain than for a diffuse microdomain. This proximity may increase the cross-linking efficiency, leading to a greater modulus. Finally, because the IL/PEG 8000 blend was cross-linked through discrete cross-linked molecular junctions rather than cross-linked microdomains, the reinforcement mechanism is somewhat different and thus these gels cannot be directly compared to the BCP gels.

Ionic Conductivity. The ionic conductivities of the cross-linked blends were measured in order to demonstrate the potential for these materials to be used as solid polymer electrolytes and to determine the effect of BCP phase behavior. Figure 4 compares the ionic conductivities of the cross-linked polymer blends and the neat IL. There was a clear decrease in ionic conductivity between the cross-linked IL/polymer blends and the neat IL, and the conductivity of the 50/50 blends was clearly less than the 80/20 blends, due to a reduced number of charge carriers. However, the ionic conductivities of the IL/polymer blends at equivalent IL compositions were all very close in value, making it difficult to discern any difference.

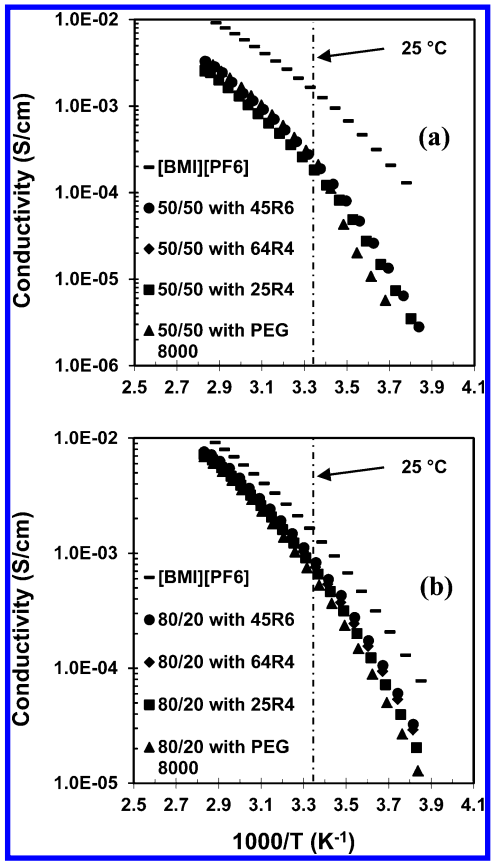

Figure 4. Ionic conductivities of the neat IL and cross-linked polymer gels, for (a) 50/50 IL/polymer (w/w) blend compositions and (b) 80/20 blend compositions.

To make a more careful comparison of the polymer gel conductivities, the ionic conductivity for each gel at 25 °C was estimated by cubic interpolation and tabulated below in Table 2. The 90/10 with 45R6 cross-linked blend had very high ionic conductivity, exceeding 1.0 mS/cm (at 25 °C). The conductivities of the un-cross-linked blends are also shown, and it is apparent that the ionic conductivity does not change significantly upon cross-linking. This demonstrates that these blends can be mechanically reinforced by cross-linking without loss of conductivity.

Table 2. Ionic Conductivity (σ) in mS/cm ($\times 10^{-3}$ S/cm) at 25 °C of [BMI][PF_6]/Polymer Blends, before and after Cross-Linking, and Estimated Volume Fraction of the Combined PEO and IL Microphase (ϕ_{PEO+IL})

composition	un-cross-linked σ	cross-linked σ	ϕ_{PEO+IL}
[BMI][PF_6]	**1.49** ± 0.14	–	–
90/10 w/ 45R6	**1.24** ± 0.02	**1.22** ± 0.01	0.95
80/20 w/ PEG 8000	**0.69** ± 0.03	**0.64** ± 0.05	1.00
80/20 w/ 25R4	**0.61** ± 0.01	**0.61** ± 0.05	0.85
80/20 w/ 45R6	**0.79** ± 0.06	**0.76** ± 0.09	0.91
80/20 w/ 64R4	**0.76** ± 0.01	**0.83** ± 0.11	0.85
50/50 w/ PEG 8000	**0.21** ± 0.05	**0.23** ± 0.01	1.00
50/50 w/ 25R4	**0.24** ± 0.02	**0.14** ± 0.04	0.65
50/50 w/ 45R6	**0.25** ± 0.01	**0.22** ± 0.01	0.78
50/50 w/ 64R4	**0.37** ± 0.01	**0.31** ± 0.01	0.66

[a]There is some uncertainty in the morphology, but the most likely arrangement is indicated.

dx.doi.org/10.1021/ma401302r | Macromolecules 2013, 46, 9313–9323

Despite blending with 50 wt % of the IL, the 50/50 with 45R6 blends and 50/50 with PEG 8000 blends still exhibit some residual crystallinity. The conductivity of these blends is noticeably lower than the fully amorphous 50/50 with 64R4 blend, although the difference is not very large. It is possible the PEO crystallization is not substantial enough to greatly impact ion transport.

The conductivity of the blends, cross-linked and un-cross-linked, was not highly dependent on the BCP used or gel morphology. The differences in conductivity were small, regardless if the blend was a single phase (PEG 8000 blends), weakly microphase separated (25R4 blends), or strongly microphase separated (64R4, 45R6 blends), suggesting that the properties of the IL have the most significant influence on conductivity at high IL loadings (greater than 50%). There was also no substantial difference with variations in BCP composition, approximately 40 wt % PEO for 25R4 and 64R4, and 64 wt % for 45R6.

These findings are in contrast to several reports in the literature, which show very large (orders of magnitude) changes in conductivity with varying phase behavior for BCP electrolytes having conducting and nonconducting blocks. Several works have compared the ionic conductivity of microphase separated BCPs with random, phase-mixed copolymers.[36,48,57] All have reported far greater conductivity for microphase separated BCPs.[36] There seems to be a clear indication that microphase separation enhances ionic conductivity. BCPs having weak microphase separation of conducting and nonconducting blocks have also been investigated, for which increasing the microphase separation strength was observed to enhance the ionic conductivity.[35,46,58]

Other works have investigated the effect of BCP morphology. These reports have found that transitioning from a cylindrical morphology in which the conducting block is the minority microphase to either a cubic bicontinuous[38] or lamellar morphology[55] results in a dramatic increase in conductivity. The superiority of BCP electrolytes having a bicontinuous conducting microdomain has also been reported.[46,60] This is due to an increase in connectivity between the microdomains of the ion-conducting block, providing a less tortuous path for ion conduction. Similarly, transitioning from a lamellar morphology to a mixed lamellar/cylindrical morphology also achieves a large increase in conductivity[54] by further increasing connectivity between conducting microdomains. Other works also emphasize the importance of BCP morphology, demonstrating that microdomain orientation has a substantial impact on conductivity.[45,50]

Here, the conducting microphase (PEO/IL) was the majority phase for each BCP/IL blend investigated due to the relatively high loading of IL that was required to suppress PEO crystallization. Thus, a continuous pathway for ion conduction was always assured regardless of the blend, resulting in the observed near invariance in ionic conductivity with BCP composition.

In contrast to much of the literature, there was little variance in conductivity with microphase separation strength. IL/25R4 blends, despite having very weak microphase separation strength, had nearly the same conductivity as the strongly separated IL blends with 45R6 and 64R4. The results of the conductivity measurements on the PEG 8000 gels further demonstrate the limited dependence of ionic conductivity on phase behavior in these mixtures. For the PEG 8000 blends, there was only a single, mixed phase of PEO/IL. Despite the lack of phase separation, the conductivity of IL/PEG 8000 blends was nearly the same as that of the IL/BCP gels. It appears that microphase separation of the BCP blends does not impart any substantial conductivity gain compared to PEG 8000 blends.

The present report also contrasts the literature in an additional way. Several previous works have found that microphase separation led to an increase in the local concentration of charge carriers in the conducting block, increasing ionic conductivity.[50,57,62,83] Considering this, it would seem that in the present work, microphase separation should result in a higher effective IL concentration in the conducting microphases of the IL/BCP gels compared to the IL/PEG 8000 gel. However, this was not observed. The reason for this difference is not clear, although the present mixtures do vary from those investigated previously in several ways. For example, in several of the cited works,[57,62] the conducting block is below its T_g, whereas here PEO is well above its T_g (average reported value of 200 K).[84] Perhaps the effect of local ion concentration is not as significant when the conducting midblock is far above its T_g. Also, in another report it was concluded that charge carrier localization minimized the retardation effect on ion transport from the interface with the glassy PS microdomain.[83] In the present case, the PPO microdomain is not glassy, nor is the cross-linking particularly dense, and thus an ion localization effect may again have a reduced impact.

Despite BCP microphase separation not presenting any substantial benefit for the present systems, it may still be possible to obtain greater mechanical strength while maintaining high conductivity by using a BCP, as the literature has suggested.[35,43,49,52] Here, the DMA results (Figure 3) show that the strongly microphase separated blends had higher moduli than the PEG 8000 blend, 33% greater for blends with 64R4 and 66% for blends with 45R6. It may be possible to further enhance the moduli by using an additional cross-linker molecule. BCP microphase separation can be used to isolate this molecule from the conducting microphase, allowing mechanical strength to be increased without a corresponding decrease in ionic conductivity. This possibility was examined by introducing cross-linker molecules which were phase selective for either the PPO microphase or the PEO/IL microphase.

Phase Selective Cross-Linkers. The cross-linkers in this work were PPO and PEO oligomers (with degrees of polymerization n = 11−12 and n = 13−14 respectively) with cross-linking acrylate end groups (Figure 5). The PPO−acrylate was found to be immiscible in the IL, whereas the PEO−acrylate was fully miscible in the IL. Therefore, the PPO−acrylate was selective for the PPO blocks, and was expected to cross-link only in the PPO microdomain upon UV exposure.

The blends having oligomeric cross-linkers are referred to by the parts by weight of the components present. For example, 80/20/10 with 45R6/PEO−acrylate refers to the blends having 80 parts IL (by weight), 20 parts 45R6, and 10 parts PEO−diacrylate cross-linker.

The phase behavior of 80/20/10 and 90/10/05 with 45R6 blends having PEO− and PPO−acrylate cross-linkers was investigated to ensure that strong microphase separation was maintained when the cross-linkers are included. Figure 5 shows the SAXS profiles of these blends, before and after cross-linking. The un-cross-linked blends having both PEO−acrylate and PPO−acrylate cross-linkers were strongly microphase

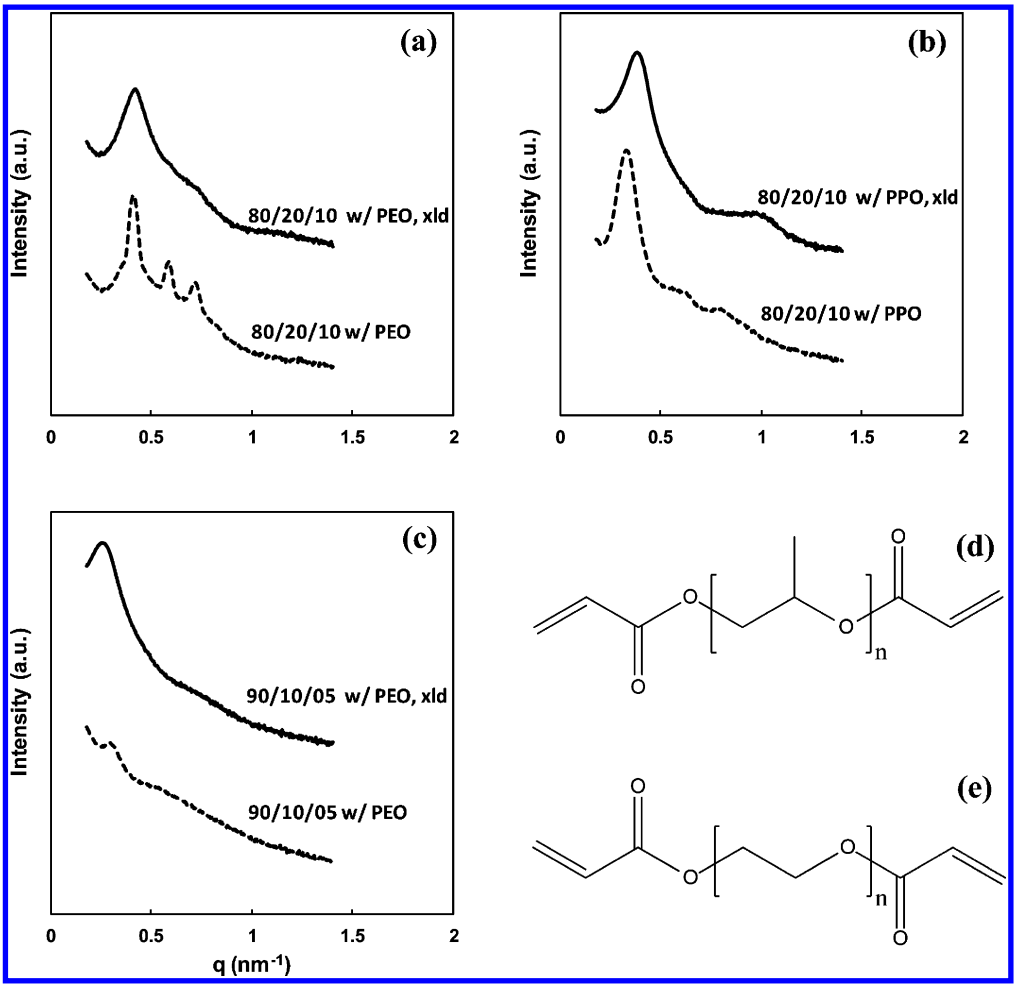

Figure 5. SAXS profiles of IL/45R6/cross-linker blends, both before and after cross-linking (xld), for the (a) 80/20/10 (w/w/w) blends with PEO-acrylate, (b) 80/20/10 blends with PPO-acrylate, and (c) 90/10/05 blends with PPO-acrylate. All SAXS profiles were obtained at 80 °C. Also shown are structures of the (d) PPO-acrylate cross-linker and the (e) PEO-acrylate cross-linkers.

separated. In the blend with PEO−acrylate, there was a clear spherical morphology (q_1: $2^{1/2}q_1$: $3^{1/2}q_1$:$4^{1/2}$). In the blend with PPO−acrylate, there was a q_1: $1.8q_1$: $2.4q_1$ ratio of scattering peaks, which does not correspond to any particular BCP morphology. The intensities of the higher order peaks were subdued, complicating the determination of peak locations and perhaps resulting in this uncharacteristic ratio of scattering peaks. The SAXS profile for the un-cross-linked 90/10/05 with 45R6/PPO−acrylate blend showed weak microphase separation. As before, these morphologies became distorted after cross-linking, but clear primary peaks remained, indicating that the BCP/IL/cross-linker blends remained strongly microphase separated.

To examine the effect of including the cross-linking oligomers on the mechanical properties, DMA was again used to measure the dynamic storage moduli of the cross-linked blends. The results showed that these cross-linkers can substantially increase the mechanical strength. The 80/20/10 with PEG 8000/PEO−acrylate blend had the highest modulus (approximately 600 kPa at 0.02 Hz), about a 5-fold increase compared to the 80/20 with PEG 8000 blend where the cross-linker was absent (120 kPa at 0.02 Hz). The PEO−acrylate cross-linker has a much lower molecular weight between cross-linking end groups than PEG 8000 (degree of polymerization n = 11−12 and molecular weight of 700 g/mol for the oligomer, vs n = 180 and 8000 g/mol for PEG 8000), and thus cross-link density was increased, increasing the modulus. The 80/20/10 blend with 45R6/PEO−acrylate showed the next highest modulus, with an approximately 2.5-fold increase over the 80/20 blend (530 kPa compared to 200 kPa). The increase in modulus for the 45R6 blend was less when the PPO−acrylate cross-linker was used, approximately a 2-fold increase (400 kPa compared to 200 kPa). Most likely this was due to cross-links only being formed in the PPO minority blocks, maintaining nearly the same molecular weight between cross-links across the whole of the gel and only affecting an increase cross-link density inside PPO microdomains. In comparison, the PEO−acrylate cross-linker is selective for the PEO/IL block, and thus cross-links were formed throughout the majority of the gel, increasing cross-link density across the whole gel. The 90/10/05 with 45R6/PPO−acrylate blend had the lowest modulus, although there was a still a 2-fold increase compared to the 90/10 with 45R6 blend in which the cross-linker was not included (40 kPa compared to 20 kPa).

Compared to other reports of IL/polymer gels at high IL concentrations (>50 wt %), the moduli reported here (Figure 6) are fairly high. With a 50 wt % concentration of IL, storage moduli of 100−200 kPa were reported.[52] At IL concentrations near those reported here (75−90 wt %), moduli are on the order of 1−10 kPa,[51,56] with one report showing moduli up to

dx.doi.org/10.1021/ma401302r | Macromolecules 2013, 46, 9313−9323

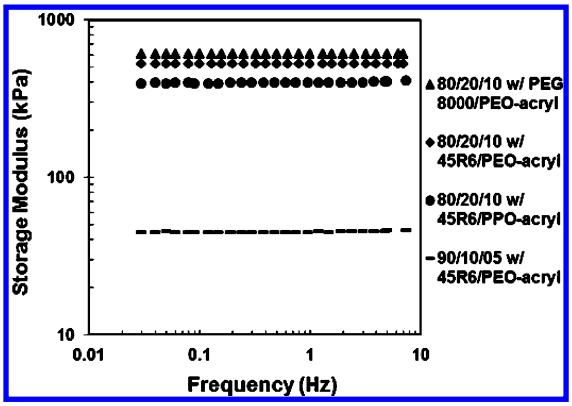

Figure 6. Compressive storage moduli of the cross-linked IL/polymer/cross-linker gels as function of frequency.

4.5 MPa.[22] It is important to note that different characterization methods result in varying measures of moduli (i.e., storage moduli in shear are less than storage moduli in compression). However, our results clearly demonstrate the present approach achieves substantial mechanical reinforcement.

Lastly, the ionic conductivity for blends with the cross-linkers present was examined, as shown in Figure 7. The conductivities

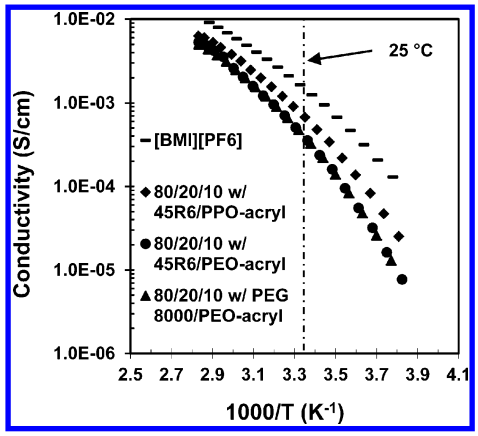

Figure 7. Ionic conductivities of the neat IL and cross-linked polymer gels, for 80/20/10 IL/polymer/cross-linker blend compositions, using either the PPO-acrylate or PEO-acrylate cross-linker.

of each blend are still fairly close, although it is noticeably lower for blends with the PEO−acrylate cross-linker. The ionic conductivities at 25 °C, both before and after cross-linking, have been estimated by cubic interpolation and are summarized in Table 3 for ease of comparison.

Before cross-linking, there was no substantial difference in conductivity between blends having either PPO−acrylate or PEO−acrylate. However, after cross-linking, the conductivity for blends with the PEO−acrylate cross-linker was decreased by 40−45%. Whereas for blends having the PPO−acrylate cross-linker, there was no significant change in ionic conductivity.

Table 3. Ionic Conductivity (σ) in mS/cm ($\times 10^{-3}$ S/cm) at 25 °C of [BMI][PF_6]/Polymer/Cross-Linker Blends, before and after Cross-Linking

composition	un-cross-linked σ	cross-linked σ
[BMI][PF_6]	**1.49** ± 0.14	–
80/20/10 w/ 45R6/PPO−acrylate	**0.68** ± 0.01	**0.64** ± 0.05
80/20/10 w/ 45R6/PEO−acrylate	**0.60** ± 0.01	**0.35** ± 0.07
80/20/10 w/ PEG 8000/PEO−acrylate	**0.56** ± 0.03	**0.32** ± 0.07
90/10/05 w/ 45R6/PPO−acrylate	**0.93** ± 0.01	**0.98** ± 0.01

Because PEO−acrylate is selective for the PEO/IL microphase, cross-linking resulted in the formation a rigid network primarily in this microphase. The introduction of the oligomeric PEO−acrylate into the blends drastically increases the cross-link density compared to the IL/PEG 8000 blends not having additional cross-linker. Therefore, there is a much greater retardation effect on the segmental dynamics of the PEO chains for blends having the additional PEO−diacrylate cross-linker. This in turn causes a noticeable decrease in ionic conductivity. Segmental dynamics must be similarly slowed for IL/45R6 blends having the PEO−acrylate cross-linker. Conversely, the PPO−acrylate cross-linker was instead selective for the PPO microphase and the cross-linked network remained confined to this microphase after the cross-linking reaction. Therefore, in the case of high cross-link density, microphase separation becomes beneficial, as compared to the prior results where cross-link density was far lower and thus isolation of the cross-links had little impact, demonstrated by the near invariance in conductivity for IL/PEG 8000 blends compared to the microphase separated blends.

These results are consistent with the findings of Zhang et al., in which the ionic conductivity of ABA-type poly(styrene)−poly(methyl methacrylate)−poly(styrene) BCP gels was found to be decoupled from the mechanical stability provided by the glassy poly(styrene) blocks.[52] In another work, it was found that increasing molecular weight of the PEO block resulted in an increase in both the storage modulus and ionic conductivity, also decoupling mechanical strength and ionic conductivity.[38] In the present case, this decoupling was achieved by isolating the cross-link points of a chemically cross-linked microphase separated gel within the minor, nonconducting domain. This represents an additional, additive-driven strategy for mechanical property enhancement without incurring a large sacrifice in conductivity.

■ CONCLUSIONS

Highly conductive, mechanically stable gels were fabricated from cross-linkable PPO−PEO−PPO triblock copolymers and cross-linkable PEO homopolymers. Blending the polymers with the ionic liquid [BMI][PF_6] inhibited their crystallization, enabling rapid ion transport. The ionic liquid also induced strong microphase separation in the triblock copolymers, which were otherwise disordered or weakly ordered in the melt. Cross-linking these blends yielded solid, elastic gels. Despite variances in phase behavior with the choice of polymer, there was very little difference observed in the ionic conductivity between blends with the same ionic liquid loadings. However, it was found that microphase separation can be used to increase mechanical stability without detriment to the ionic conductivity, by isolating phase-selective photoreactive cross-linkers from the conducting phase. Therefore, although block copolymer microphase separation cannot be used for the present materials to substantially enhance ionic conductivity, it does allow mechanical stability and conductivity to be decoupled. This in turn will allow polymer electrolytes constructed using this method to achieve both high ionic conductivity and high mechanical strength.

dx.doi.org/10.1021/ma401302r | Macromolecules 2013, 46, 9313−9323

■ ASSOCIATED CONTENT

Supporting Information

Polymer synthesis, polymer end group modification, and photocalorimetry. This material is available free of charge via the Internet at http://pubs.acs.org.

■ AUTHOR INFORMATION

Corresponding Authors

*E-mail: (T.P.R.) russell@mail.pse.umass.edu.
*E-mail: (J.J.W. watkins@polysci.umass.edu.

Notes

The authors declare no competing financial interest.

■ ACKNOWLEDGMENTS

This work was supported by the NSF-supported Materials Research Science and Engineering Center on Polymers (DMR-0820506) and the Center for Hierarchical Manufacturing (CMMI-1025020) at the University of Massachusetts Amherst.

■ REFERENCES

(1) Smitha, B.; Sridhar, S.; Khan, A. A. *J. Membr. Sci.* **2005**, *259*, 10−26.
(2) Li, B.; Wang, L.; Kang, B.; Wang, P.; Qiu, Y. *Sol. Energy Mater. Sol. Cells* **2006**, *90*, 549−573.
(3) Lewandowski, A.; Zajder, M.; Frackowiak, E.; Beguin, F. *Electrochim. Acta* **2001**, *46*, 2777−2780.
(4) Tarascon, J. M.; Armand, M. *Nature* **2001**, *414* (6861), 359−367.
(5) Kang, X. *Chem. Rev.* **2005**, *104*, 4303−4417.
(6) Meyer, W. *Adv. Mater.* **1998**, *10*, 439−448.
(7) Goodenough, J. B.; Kim, Y. *Chem. Mater.* **2010**, *22* (3), 587−603.
(8) Berthier, C.; Gorecki, W.; Minier, M.; Armand, M. B.; Chabagno, J. M.; Rigaud, P. *Solid State Ionics* **1983**, *11* (1), 91−95.
(9) Robitaille, C. D.; Fauteux, D. *J. Electrochem. Soc.* **1986**, *133* (2), 315−325.
(10) Lee, S.-I.; Schomer, M.; Peng, H.; Page, K. A.; Wilms, D.; Frey, H.; Soles, C. L.; Yoon, D. Y. *Chem. Mater.* **2011**, *23*, 2685−2688.
(11) Lascaud, S.; Perrier, M.; Vallee, A.; Besner, S.; Prudhomme, J.; Armand, M. *Macromolecules* **1994**, *27* (25), 7469−7477.
(12) Weingaertner, H. *Angew. Chem., Int. Ed.* **2008**, *47* (4), 654−670.
(13) Qian, X. M.; Gu, N. Y.; Cheng, Z. L.; Yang, X. R.; Wang, E. K.; Dong, S. J. *Mater. Chem. Phys.* **2002**, *74* (1), 98−103.
(14) Chintapalli, S.; Frech, R. *Macromolecules* **1996**, *29* (10), 3499−3506.
(15) Lee, H. S.; Yang, X. Q.; McBreen, J.; Xu, Z. S.; Skotheim, T. A.; Okamoto, Y. *J. Electrochem. Soc.* **1994**, *141* (4), 886−889.
(16) Shin, J. H.; Henderson, W. A.; Passerini, S. *Electrochem. Commun.* **2003**, *5* (12), 1016−1020.
(17) Lewandowski, A.; Swiderska, A. *Solid State Ionics* **2004**, *169* (1−4), 21−24.
(18) Castiglione, F.; Ragg, E.; Mele, A.; Appetecchi, G. B.; Montanino, M.; Passerini, S. *J. Phys. Chem. Lett.* **2011**, *2*, 153−157.
(19) Choi, J. W.; Cheruvally, G.; Kim, Y. H.; Kim, J. K.; Manuel, J.; Raghavan, P.; Ahn, J. H.; Kim, K. W.; Ahn, H. J.; Choi, D. S.; Song, C. E. *Solid State Ionics* **2007**, *178* (19−20), 1235−1241.
(20) Kumar, D.; Hashmi, S. A. *Solid State Ionics* **2010**, *181* (8−10), 416−423.
(21) Liu, S.; Imanishi, N.; Zhang, T.; Hirano, A.; Takeda, Y.; Yamamoto, O.; Yang, J. *J. Electrochem. Soc.* **2010**, *157* (10), A1092−A1098.
(22) Sterner, E. S.; Rosol, Z. P.; Gross, E. M.; Gross, S. M. *J. Appl. Polym. Sci.* **2009**, *114* (5), 2963−2970.
(23) Tiyapiboonchaiya, C.; MacFarlane, D. R.; Sun, J. Z.; Forsyth, M. *Macromol. Chem. Phys.* **2002**, *203* (13), 1906−1911.
(24) Bansal, D.; Cassel, F.; Croce, F.; Hendrickson, M.; Plichta, E.; Salomon, M. *J. Phys. Chem. B* **2005**, *109* (10), 4492−4496.
(25) Fuller, J.; Breda, A. C.; Carlin, R. T. *J. Electroanal. Chem.* **1998**, *459* (1), 29−34.
(26) Kim, J. K.; Matic, A.; Ahn, J. H.; Jacobsson, P. *J. Power Sources* **2010**, *195* (22), 7639−7643.
(27) Nakagawa, H.; Izuchi, S.; Kuwana, K.; Nukuda, T.; Aihara, Y. *J. Electrochem. Soc.* **2003**, *150* (6), A695−A700.
(28) Gerbaldi, C.; Nair, J. R.; Ahmad, S.; Meligrana, G.; Bongiovanni, R.; Bodoardo, S.; Penazzi, N. *J. Power Sources* **2010**, *195* (6), 1706−1713.
(29) Koh, J. H.; Koh, J. K.; Park, N. G.; Kim, J. H. *Sol. Energy Mater. Sol. Cells* **2010**, *94* (3), 436−441.
(30) Rupp, B.; Schmuck, M.; Balducci, A.; Winter, M.; Kern, W. *Eur. Polym. J.* **2008**, *44* (9), 2986−2990.
(31) Kim, G. T.; Appetecchi, G. B.; Carewska, M.; Joost, M.; Balducci, A.; Winter, M.; Passerini, S. *J. Power Sources* **2010**, *195* (18), 6130−6137.
(32) Ghosh, A.; Wang, C.; Kofinas, P. *J. Electrochem. Soc.* **2010**, *157*, A846−A849.
(33) Gopinadhan, M.; Majewski, P. W.; Osuji, C. O. *Macromolecules* **2010**, *43*, 3286−3293.
(34) Niitani, T.; Shimada, M.; Kawamura, K.; Dokko, K.; Rho, Y. H.; Kanamura, K. *Electrochem. Solid-State Lett.* **2005**, *8* (8), A385−A388.
(35) Panday, A.; Mullin, S. A.; Gomez, E. D.; Wanakule, N. S.; Chen, V. L.; Hexemer, A.; Pople, J. A.; Balsara, N. P. *Macromolecules* **2009**, *42*, 4632−4637.
(36) Ruzette, A. V. G.; Soo, P. P.; Sadoway, D. R.; Mayes, A. M. *J. Electrochem. Soc.* **2001**, *148* (6), A537−A543.
(37) Soo, P. P.; Huang, B. Y.; Jang, Y. I.; Chiang, Y. M.; Sadoway, D. R.; Mayes, A. M. *J. Electrochem. Soc.* **1999**, *146* (1), 32−37.
(38) Cho, B. K.; Jain, A.; Gruner, S. M.; Wiesner, U. *Science* **2004**, *305* (5690), 1598−1601.
(39) Singh, M.; Odusanya, O.; Wilmes, G. M.; Eitouni, H. B.; Gomez, E. D.; Patel, A. J.; Chen, V. L.; Park, M. J.; Fragouli, P.; Iatrou, H.; Hadjichristidis, N.; Cookson, D.; Balsara, N. P. *Macromolecules* **2007**, *40* (13), 4578−4585.
(40) Wanakule, N. S.; Panday, A.; Mullin, S. A.; Gann, E.; Hexemer, A.; Balsara, N. P. *Macromolecules* **2009**, *42* (15), 5642−5651.
(41) Higa, M.; Fujino, Y.; Koumoto, T.; Kitani, R.; Egashira, S. *Electrochim. Acta* **2005**, *50*, 3832−3837.
(42) Kim, B.; Ahn, H.; Kim, J. H.; Ryu, D. Y.; Kim, J. *Polymer* **2009**, *50* (15), 3822−3827.
(43) Kosonen, H.; Valkama, S.; Hartikainen, J.; Eerikainen, H.; Torkkeli, M.; Jokela, K.; Serimaa, R.; Sundholm, F.; ten Brinke, G.; Ikkala, O. *Macromolecules* **2002**, *35*, 10149−10154.
(44) Ryu, S. W.; Trapa, P. E.; Olugebefola, S. C.; Gonzalez-Leon, J. A.; Sadoway, D. R.; Mayes, A. M. *J. Electrochem. Soc.* **2005**, *152* (1), A158−A163.
(45) Young, W. S.; Epps, T. H. *Macromolecules* **2012**, *45*, 4689−4697.
(46) Mullin, S. A.; Teran, A. A.; Yuan, R.; Balsara, N. P. *J. Polym. Sci., Part B: Polym. Phys.* **2013**, *51*, 927−934.
(47) Lee, J. W.; Hong, S. M.; Kim, J.; Koo, C. M. *Sens. Actuators B* **2012**, *162*, 369−376.
(48) Kim, S. K.; Kim, D. G.; Lee, A.; Sohn, H. S.; Wie, J. J.; Nguyen, N. A.; Mackay, M. E.; Lee, J. C. *Macromolecules* **2012**, *45*, 9347−9356.
(49) Niitani, T.; Amaiki, M.; Nakano, H.; Dokko, K.; Kanamura, K. *J. Electrochem. Soc.* **2009**, *156*, A577−A583.
(50) Gwee, L.; Choi, J. H.; Winey, K. I.; Elabd, Y. A. *Polymer* **2010**, *51*, 5516−5524.
(51) Imaizumi, S.; Kokubo, H.; Watanabe, M. *Macromolecules* **2012**, *45*, 401−409.
(52) Zhang, S.; Lee, K. H.; Frisbie, C. D.; Lodge, T. P. *Macromolecules* **2011**, *44*, 940−949.
(53) Naidu, S.; Ahn, H.; Gong, J.; Kim, B.; Ryu, D. Y. *Macromolecules* **2011**, *44*, 6085−6093.
(54) Simone, P. M.; Lodge, T. P. *ACS Appl. Mater. Interfaces* **2009**, *1* (12), 2812−2820.
(55) Weber, R. L.; Ye, Y.; Schmitt, A. L.; Banik, S. M.; Elabd, Y. A.; Mahanthappa, M. K. *Macromolecules* **2011**, *44*, 5727−5735.

(56) He, Y. Y.; Boswell, P. G.; Buhlmann, P.; Lodge, T. P. *J. Phys. Chem. B* **2007**, *111* (18), 4645−4652.
(57) Ye, Y.; Choi, J. H.; Winey, K. I.; Elabd, Y. A. *Macromolecules* **2012**, *45*, 7027−7035.
(58) Choi, J. H.; Ye, Y.; Elabd, Y. A.; Winey, K. I. *Macromolecules* **2013**, *46*, 5290−5300.
(59) Green, M. D.; Choi, J. H.; Winey, K. I.; Long, T. E. *Macromolecules* **2012**, *45*, 4749−4757.
(60) Kim, O.; Kim, S. Y.; Ahn, H.; Kim, C. W.; Rhee, Y. M.; Park, M. J. *Macromolecules* **2012**, *45*, 8702−8713.
(61) Kim, O.; Jo, G.; Park, Y. J.; Kim, S.; Park, M. J. *J. Phys. Chem. Lett.* **2013**, *4*, 2111−2117.
(62) Hoarfrost, M. L.; Segalman, R. A. *Macromolecules* **2011**, *44*, 5281−5288.
(63) Bates, F. S.; Fredrickson, G. H. *Phys. Today* **1999**, *52* (2), 32−38.
(64) Matsen, M. W.; Bates, F. S. *Macromolecules* **1996**, *29*, 1091−1098.
(65) Sanabria-DeLong, N.; Crosby, A. J.; Tew, G. N. *Biomacromolecules* **2008**, *9* (10), 2784−2791.
(66) Chun, K. W.; Lee, J. B.; Kim, S. H.; Park, T. G. *Biomaterials* **2005**, *26*, 3319−3326.
(67) Lee, J. I.; Kim, H. S.; Yoo, H. S. *Int. J. Pharm.* **2009**, *373*, 93−99.
(68) Nardin, C.; Hirt, T.; Leukel, J.; Meier, W. *Langmuir* **2000**, *16* (3), 1035−1041.
(69) Hong, S.; Yang, L. Z.; MacKnight, W. J.; Gido, S. P. *Macromolecules* **2001**, *34* (20), 7009−7016.
(70) Miranda, D. F.; Russell, T. P.; Watkins, J. J. *Macromolecules* **2010**, *43*, 10528−10535.
(71) Kim, S.; Park, S.-J. *Electrochim. Acta* **2009**, *54*, 3775−3780.
(72) Kim, K. S.; Lee, S. B.; Lee, H.; Kim, H. S.; Lee, Y.; Kwack, K. *J. Ind. Eng. Chem.* **2009**, *15* (5), 657−660.
(73) Kovacs, A. J.; Gonthier, A.; Straupe, C. *J. Polym. Sci., Part C: Polym. Symp.* **1975**, *50*, 283−325.
(74) Kovacs, A. J.; Straupe, C.; Gonthier, A. *J. Polym. Sci., Part C: Polym. Symp.* **1977**, *59*, 31−54.
(75) Zhang, F.; Stuhn, B. *Colloid Polym. Sci.* **2007**, *285*, 371−379.
(76) Tirumala, V. R.; Romang, A.; Agarwal, S.; Lin, E. K.; Watkins, J. J. *Adv. Mater.* **2008**, *20* (9), 1603−1608.
(77) Fairclough, J. P. A.; Yu, G.-E.; Mai, S.-M.; Crothers, M.; Mortensen, K.; Ryan, A. J.; Booth, C. *Phys. Chem. Chem. Phys.* **2000**, *2*, 1503−1507.
(78) Virgili, J. M.; Hexemer, A.; Pople, J. A.; Balsara, N. P.; Segalman, R. A. *Macromolecules* **2009**, *42* (13), 4604−4613.
(79) Zhang, G. D.; Chen, X.; Zhao, Y. R.; Ma, F. M.; Jing, B.; Qiu, H. Y. *J. Phys. Chem. B* **2008**, *112* (21), 6578−6584.
(80) Gomez, E. D.; Das, J.; Chakraborty, A. K.; Pople, J. A.; Balsara, N. P. *Macromolecules* **2006**, *39*, 4848−4859.
(81) Russell, T. P.; Karis, T. E.; Gallot, Y.; Mayes, A. M. *Nature* **1994**, *368*, 729−731.
(82) Kavanagh, G. M.; Ross-Murphy, S. B. *Prog. Polym. Sci.* **1998**, *23*, 533−562.
(83) Gomez, E. D.; Panday, A.; Feng, E. H.; Chen, V.; Stone, G. M.; Minor, A. M.; Kisielowski, C.; Downing, K. H.; Borodin, O.; Smith, G. D.; Balsara, N. P. *Nano Lett.* **2009**, *9*, 1212−1216.
(84) Mark, J. E. *Polymer Data Handbook*. Oxford University Press, Inc.: Oxford, U.K., 1999.